New Dinuclear 5-*ansa*-Lanthanocene Derivatives. Crystal Structures of $[Ln\{2,6\text{-}(CH_2C_5H_4)_2C_5H_3N\}\mu\text{-}O_2SOCF_3]_2$ (Ln = Nd, Y, Yb) and a VT Solution NMR (^1H, ^{19}F) Study of the Fluxional Yttrium Homologue

Gino Paolucci,*,† Jacopo Zanon,† Vittorio Lucchini,‡ Wulf-Erich Damrau,§ Eric Siebel,§ and R. Dieter Fischer§

Dipartimento di Chimica and Dipartimento di Scienze Ambientali, Università Ca' Foscari di Venezia, Dorsoduro 2137, I-30123 Venezia, Italy, and Institut für Anorganische und Angewandte Chemie, Universität Hamburg, Martin-Luther-King Platz 6, D-20146 Hamburg, Germany

Received June 7, 2001

Five homologues of the new complex series $[LnL(\mu\text{-OTf})]_2$ with Ln = Pr (**1**), Nd (**2**), Sm (**3**), Y (**4**), Yb (**5**) have been prepared from $[Ln(OTf)_3]$ and Na_2L, where L designates two cyclopentadienyl rings tethered by a 2,6-bis(methylene)pyridyl unit and −OTf the triflate (trifluoromethanesulfonate) anion. According to crystal structure analyses of **2**, **4**, and **5**, each triflate ligand bridges two Ln ions (Ln−O−S(O)−O′−Ln′), while, owing to substantial Ln−N(pyridyl) bonding, the LnL fragments turn out to be notably rigid entities. Nevertheless, the variable-temperature (VT) ^1H NMR spectra of all complexes reveal notable fluxionality. According to a detailed VT ^{19}F NMR study of **4**, two dinuclear isomers, differing in the trans and cis orientations, respectively, of their two L fragments, interconvert with a negligibly small entropy of activation $\Delta S^{\ddagger}$. A motion reminiscent of the Berry turnstile would most plausibly explain the experimental findings.

1. Introduction

Metallocenophane complexes with a five-membered tether containing the centrally located Lewis base B (Figure 1) are particularly well conditioned for an ancillary B→M interaction.[1] If, moreover, the three central atoms of the tether would become part of a rigid cyclic entity (dotted lines in Figure 1), the metallocenophane in total is expected to gain optimal rigidity. This situation is very desirable, inter alia, for spectroscopic studies of complexes of the f elements, where facile ligand rearrangement is very common. In d transition metal chemistry, one quite extensively considered tether to date is the 2,6-dimethylpyridinediyl unit. So far, only one 5f and one rare earth metal complex (i.e. with M = Y,[1] U[2] and with the ligand L = $2,6\text{-}(CH_2C_5H_4)_2C_5H_3N$) have been structurally characterized by X-ray diffraction. Genuine lanthanide (4f) metal complexes mainly of the types $[LnL(\mu\text{-Cl})]_2$ and $[(LnL)_2(\mu\text{-L})]$ have successfully been studied by ^1H NMR spectroscopy in solution,[3] while so far all attempts to arrive at single crystals have failed. In the present contribution, several new *triflato* complexes of the composition $[LnL(\mu\text{-OTf})]_2$ (OTf = trifluoromethanesulfonate) with Ln = Pr, Nd, Sm, Y, Yb (**1**−**5**) will be described. Owing to the more favorable crystallization properties of this complex family, the first successful structure analyses of L-containing complexes involving genuine 4f elements have become possible. Moreover, systematic room-temperature and variable-temperature (VT) NMR studies of these compounds have helped in revealing several new, probably intramolecular, dynamic features.

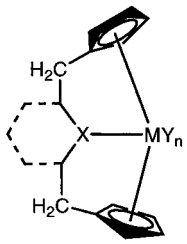

Figure 1. Schematic drawing of *ansa*-metallocenes containing in the bridging chain an additional donor atom.

2. Preparation and General Properties of the Complexes 1−5

The complexes **1**−**5** were obtained in high yields by reacting at room temperature in tetrahydrofuran the disodium salt Na_2L (L = $2,6\text{-}(CH_2C_5H_4)_2C_5H_3N$)[2] with the lanthanide triflates $[Ln(SO_3CF_3)_3]$ (Ln = Pr, Nd, Sm, Y, Yb) in the molar ratio 1:1. The air- and moisture-sensitive monotriflato complexes $[LnL(OTf)]_n$ (**1**−**5**) are

† Dipartimento di Chimica, Università Ca' Foscari di Venezia. E-mail: paolucci@unive.it.
‡ Dipartimento di Scienze Ambientali, Università Ca' Foscari di Venezia. E-mail: lucchini@unive.it.
§ Universität Hamburg.

(1) See: Damrau, W.-E.; Paolucci, G.; Zanon, J.; Siebel, E.; Fischer, R. D. *Inorg. Chem. Commun.* **1998**, *1*, 424 and references therein.
(2) Paolucci, G.; Fischer, R. D.; Benetollo, F.; Seraglia, R.; Bombieri, G. *J. Organomet. Chem.* **1991**, *412*, 327.
(3) Paolucci, G.; D'Ippolito, R.; Ye, C.; Qian, C.; Gräper, J.; Fischer, R. D. *J. Organomet. Chem.* **1994**, *471*, 97.

10.1021/om0104868 CCC: $22.00
Publication on Web 02/19/2002

Table 1. Crystal Data and Structure Refinement Parameters of the Compounds 2, 4, and 5

	2	4	5
cryst size, mm^3	0.6 × 0.55 × 0.3	0.8 × 0.6 × 0.3	0.8 × 0.6 × 0.5
empirical formula	$C_{36}H_{30}F_6N_2Nd_2O_6S_2{\cdot}2CH_2Cl_2$	$C_{36}H_{30}F_6N_2O_6S_2Y_2$	$C_{36}H_{30}F_6N_2O_6S_2Yb_2$
fw, g	1223.11	942.56	1110.82
diffractometer	Hilger & Watts Y 290	Enraf-Nonius CAD 4	Hilger & Watts Y 290
temp, K	153(2)	173(2)	153(2)
wavelength, Å	0.710 73	1.541 78	0.710 73
cryst syst	triclinic	monoclinic	monoclinic
space group	$P\bar{1}$	$C2/c$	$C2/c$
unit cell dimens			
a, Å	12.438(3)	14.156(2)	14.266(3)
b, Å	13.320(3)	15.784(3)	15.705(3)
c, Å	13.950(3)	19.276(4)	19.193(4)
α, deg	91.86(3)	90.56(2)	91.59(3)
β, deg	90.51(3)		
γ, deg	107.71(3)		
V, Å^3	2200.0(8)	4306.8(14)	4298.5(15)
Z	2	4	4
density (calcd), g/cm^3	1.828	1.454	1.716
abs coeff, cm^{-1}	27.42	51.04	44.89
F(000)	1184	1888	2136
θ range for data collection, deg	2.28−30.07	4.20−76.23	2.59−30.09
index ranges	$-1 \le h \le 17$, $-18 \le k \le 18$, $-19 \le l \le 19$	$-17 \le h \le 17$, $0 \le k \le 19$, $-8 \le l \le 24$	$-2 \le h \le 20$, $-6 \le k \le 22$, $-27 \le l \le 27$
no. of rflns collected	15 068	4680	7530
no. of indep rflns	12 900	4518	6301
max and min transmission	0.765 and 0.343	0.1846 and 0.1056	0.2124 and 0.1237
refinement method	full-matrix least squares on F^2		
data/restraints/parameters	12900/0/549	4518/0/260	6301/0/259
goodness of fit on F^2	0.743	1.808	1.051
final R indices ($I > 2\sigma(I)$)	R1 = 0.0330, wR2 = 0.1018	R1 = 0.1086, wR2 = 0.3435	R1 = 0.0616, wR2 = 0.1677
largest diff peak and hole, e/Å^3	1.845 and −1.264	3.090 and −1.762	4.223 and −3.092

Table 2. Selected Distances (Å) for 2 and 4−8

	2A/2B	7[4]	4	5	6[5]	8A/8B[6]
M(1)···M(1A)	6.1813(15)/ 6.1385(15) (Nd(2)···Nd(2A))	6.320(4)	6.1031(13)	6.0767(13)	5.581(1)	5.06/5.01
M(1)−O(1)	2.419(3) (Nd(1)−O(1A))/ 2.412(5) (Nd(2)−O(4))	2.486(3) (Nd(1)−O(2)), 2.515(3) (Nd(2)−O(3))	2.336(4)	2.301(5)	2.225(8)	2.178(7)/ 2.182(8)
M(1)−O(2A)	2.467(3) (Nd(1)−O(2))/ 2.431(3) (Nd(2)−O(5A))	2.468(3) (Nd(1)−O(1)), 2.474(3) (Nd(2)−O(4))	2.358(4)	2.347(6)	2.250(1)	2.201(8)/ 2.201(7)
M(1)−N(1)	2.635(3)/2.632(3) (Nd(2)−N(2))		2.506(4)	2.485(6)		
M(1)−Cent(1)	2.454(2)/2.4501(19) (Nd(2)−Cent(3))		2.350(3)	2.306(4)	2.277(9)	2.298
M(1)−Cent(2)	2.4497(19)/2.4418(19) (Nd(2)−Cent(4))		2.342(3)	2.303(3)	2.279(6)	2.300

dimeric. Single crystals suitable for X-ray structure analyses have so far been obtained for **2**, **4**, and **5** either by slow diffusion of *n*-hexane into concentrated toluene solutions of these complexes or just by slow cooling of concentrated solutions.

3. Crystal Structures of 2 (Ln = Nd), 4 (Ln = Y), and 5 (Ln = Yb)

Relevant crystal data and structure refinement parameters of **2**, **4**, and **5** are listed in Table 1. Despite some variation in the crystal data, the general molecular topologies are quite similar throughout. The molecules are dinuclear, in that each triflate ligand makes use of *two* of its oxygen atoms for bridging the two lanthanoid ions (molecular symmetry S_2). Eight-membered, not strictly planar, $M_2X_2O_4$ rings as present in **2**, **4**, and **5** (X = S) are quite common[4] and constitute also the structures of e.g. $[Ln(C_5H_5)_2(\mu\text{-OTf})]_2$ (Ln = Yb (**6**),[5] Lu), $[Nd(COT)(THF)_2(\mu\text{-OTf})]_2$ (**7**; COT = cyclooctatetraenide dianion, THF = tetrahydrofuran),[4] and $[Yb(C_5H_5)_2(\mu\text{-}O_2CC_6F_5)]_2$ (**8**).[6] Selected interatomic distances and angles of **2**, **4,** and **5** are collected in Tables 2 and 3 and compared with corresponding data of **6**−**8**.

The unit cell of **2** contains, like that of **8**,[6] the two similar dimers **A** and **B**. Interestingly, the molecules of **2B**, **4**−**7**, and **8A** have in common that the two Ln−O−S and Yb−O−C (**8A**) angles, respectively, involving the same Ln atom, differ considerably (Table 3), while the corresponding angles of **2A** and **8B**[6] lie closer together. Moreover, the Nd(1)−Nd(1A) distance and the S(1)−S(1A) distance in the $Nd_2S_2O_4$ ring of **2A** (Nd−Nd = 618.14(15) pm, S(1)−S(1A) = 460.87(16) pm) are slightly longer than the Nd(2)−Nd(2A) and S(2)−S(2A) distances of **2B** (613.85(15) and 455.48(15) pm, respectively). Accordingly, the distances of the sulfur atoms S(1)/S(1A) and S(2)/S(2A), respectively, from the best planes spanned by the neodymium and oxygen atoms of **2A** and **2B** differ significantly (**2A**, 140.76 pm; **2B**, 208.45 pm), indicating clearly that the shorter Nd···Nd separation in **2B** is accompanied by more pronounced ring puckering.

(4) See: Kilimann, U.; Schäfer, M.; Herbst-Irmer, R.; Edelmann, F. T. *J. Organomet. Chem.* **1994**, *469*, C10.
(5) Stehr, J.; Fischer, R. D. *J. Organomet. Chem.* **1992**, *430*, C1.
(6) Deacon, G. B.; Fallon, G. D.; MacKinnon, P. I.; Newnham, R. H.; Pain, G. N.; Tuong, T. D.; Wilkinson, D. L. *J. Organomet. Chem.* **1984**, *277*, C21.

Table 3. Selected Angles (deg) for 2 and 4−8

	2A/2B	7[4]	4	5	6[5]	8A/8B[6]
M(1)−O(1)−S(1)/Yb−O−C (for **8A** and **8B**)	168.6(2)/178.3(4) (Nd(1)−O(1A)−S(1A))/ (Nd(2)−O(4)−S(2))	149.7(2)/161.9(2) (Nd(1)−O(2)−S(2))/ (Nd(2)−O(3)−S(1))	151.1(3)	149.9(4)	158.8(6)	145(1)/150(1)
M(1)−O(2A)−S(1A)/Yb−O−C (for **8A** and **8B**)	162.03(19)/160.6(3) (Nd(1)−O(2)−S(1))/ (Nd(2)−O(5A)−S(2A))	161.7(2)/138.0(9) (Nd(1)−O(1)−S(1))/ (Nd(2)−O(4)−S(2))	157.2(2)	157.2(4)	167.2(6)	171(1)/164(1)
O(1)−M(1)−O(2A)	77.13(10)/76.86(14) (O(1A)−Nd(1)−O(2))/ (O(4)−Nd(2)−O(5A))	75.0(1)/71.8(1) (O(1)−Nd(1)−O(2))/ (O(3)−Nd(2)−O(4))	75.00(13)	74.8(2)	87.4(4)	97.4(3)/98.2(3)
Cent(1)−M(1)−Cent(2)	130.77(7)/130.89(7) (Cent(3)−Nd(2)−Cent(4))		133.56(10)	133.35(14)	131.6(1)	20/132.1
O(1)−M(1)−N(1)	76.18(9)/74.63(12) (O(1A)−Nd(1)−N(1))/ (O(4)−Nd(2)−N(2))		74.68(14)	73.94(19)		
O(2A)−M(1)−N(1)	153.14(10)/151.34(12) (O(2)−Nd(1)−N(1))/ (O(5A)−Nd(2)−N(2))		149.33(13)	148.3(2)		
Cent(1)−M(1)−O(1)	117.75(10)/113.63(18) (Cent(2)−Nd(1)−O(1A))/ (Cent(3)−Nd(2)−O(4))		116.96(15)	117.52(17)	106.3	
M(1)−N(1)−C(9)	178.45(15)/176.15(17) (Nd(2)−N(2)−C(27))		170.1(2)	171.5(3)		

Most importantly, the Ln−N distances of **2**, **4**, and **5** are consistent with genuine coordinative bonds. For instance, the Nd−N distances of **2** match well with the Nd−N distances of [Nd(η^5-C_5H_5)$_3$·C_5H_5N] (2.668(5) Å)[7] and of [Nd{OC(*t*Bu)$_3$}$_3$(MeCN)$_2$] (2.627(7) and 2.641(7) Å).[8] As complexes with notably longer Nd−N distances are also known ([Nd{$Me_2N(CH_2)_2C_5H_4$}$_2$Cl], 2.772(2) and 2.804(2) Å;[9a] [Nd{$Me_2N(CH_2)_2C_5H_4$}$_3$], 2.70(1) and 2.73(1) Å[9b]), the Nd−N interaction in **2** may be considered as comparatively strong. The Y−N distance of **4** turns out to be significantly shorter than that of its recently reported derivative [YL(μ-OH)]$_2$ (**9**, 2.621(3) Å)[1] for which Y−N bonding has also been suggested. Moreover, the Yb−N distance of **5** is shorter than in [{Yb(C_5H_5)$_3$}$_2$$\mu$-$C_4H_4N_2$] (2.61(1) Å)[10] but slightly longer than in [Yb(C_5H_5)$_3$$NCC_2H_5$] (2.414(5) Å).[11] As in **9**, the main axis of each pyridine unit is throughout collinear with the Ln−N vector (Table 3). Notable rigidity can therefore be ascribed to the two equivalent {LnL} fragments of each complex, while the {$Ln_2S_2O_4$} rings might be expected to be more flexible (vide infra). In all solid-state structures the two CF_3 groups of the μ-triflato ligands are oriented transoid and adopt equatorial positions of the $Ln_2O_4S_2$ rings, which situation corresponds to an energetically favored molecular configuration.

Some other features depending most probably on the presence, or absence, of Ln−N bonds emerge from a closer comparison of the structural data of **5** with those of **6** and **8**. For instance, both the Yb−O and Yb···Yb distances of the last two complexes are shorter than in **5** (Table 2). In contrast, the O−Yb−O angles of **6** and **8** are significantly larger than those of **5** (Table 3). No spectacular differences are, on the other hand, apparent for the Yb−Cent distances and Cent−Yb−Cent angles, respectively. Obviously, in **5** the ligands in total offer each Yb^{3+} ion formally nine electron pairs, whereas the Yb^{3+} ions of **6** and **8** participate in no more than eight electron pairs. This electron deficiency (or, alternatively seen, coordinative unsaturation) in **6** and **8** should favor the formation of slightly stronger Yb−O bonds. A similar feature might be responsible for the differences in the structural data of **2** and **7** (Ln = Nd), in that the dianionic ligand L^{2-} (seven electron pairs) is replaced in **7** by one COT^{2-} ligand (five electron pairs) and two THF donors (two electron pairs). As all of the Nd−O distances of **7** even exceed those of **2**, more efficient electron donation by the combination of COT^{2-} and two THF ligands may here be deduced. It is, on the other hand, noteworthy that in the more sterically congested complex [Ce{1,3-^{t}Bu)$_2$$C_5H_3$}$_2$($\mu$-$OSO_2$-*p*-$MeC_6H_4$)]$_2$ the sulfonato ligand uses only one of its three oxygen atoms for bridging.[12]

4. ^{1}H NMR Studies of 1−5

The room-temperature ^{1}H NMR spectrum of the diamagnetic yttrium complex **4** (Figure 5b) resembles that of the structurally confirmed[13] *mono*nuclear zirconium(IV) complex [ZrL(*n*-Bu)$_2$], in that again four C_5H_4 (Cp), two C_5H_3N (pyridyl), and one CH_2 proton resonances appear. However, from the crystal structure analysis (Figures 2−4) twice as many resonances of each fragment would be expected. Actually, several features of the room-temperature spectrum of **4** provide evidence of fluxional behavior. Thus, one of the Cp resonances (δ 6.01) is a broad singlet; the two pyridyl multiplets (one triplet at δ 7.65 and one doublet at δ 7.18) are also notably broadened, and instead of an AB type resonance

(7) Deacon, G. B.; Gatehouse, B. M.; Platts, S. N.; Wilkinson, D. L. *Aust. J. Chem.* **1987**, *40*, 907.
(8) Herrmann, W. A.; Anwander, R.; Kleine, M.; Scherer, W. *Chem. Ber.* **1992**, *125*, 1771.
(9) (a) Herrmann, W. A.; Anwander, R.; Munck, F. C.; Scherer, W. *Chem. Ber.* **1993**, *126*, 331. (b) Anwander, R.; Herrmann, W. A.; Scherer, W.; Munck, F. C. *J. Organomet. Chem.* **1993**, *462*, 163.
(10) Baker, E. C.; Raymond, K. N. *Inorg. Chem.* **1977**, *16*, 2710.
(11) Spirlet, M. R.; Rebizant, J.; Apostolidis, C.; Kanellakopulos, B. *Inorg. Chim. Acta* **1987**, *139*, 211.
(12) Gun'ko, Y. K.; Hitchcock, P. B.; Lappert, M. F. *J. Organomet. Chem.* **1995**, *499*, 213.
(13) Paolucci, G.; Lucchini, V.; Zanon, J.; Pojana, G.; Avtomonov, E. *Organometallics* **1997**, *16*, 5312.

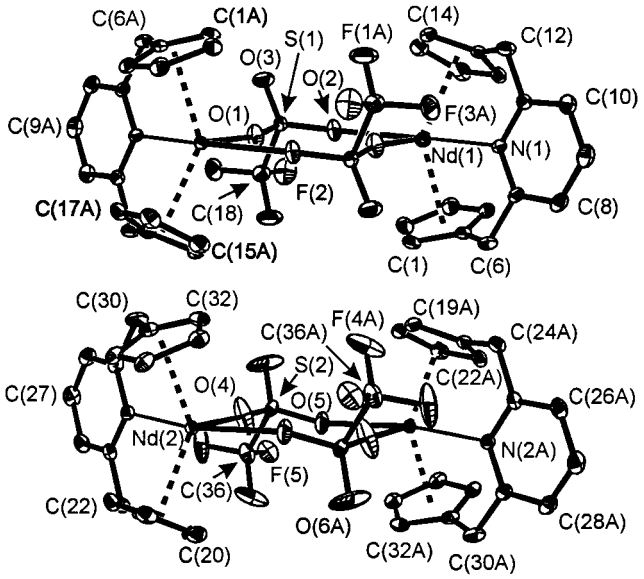

Figure 2. (A, top) Molecular structure of one of the two species of **2**, Nd[2,6-$(CH_2C_5H_4)_2$-C_5H_3N][μ-OS(O)O]$_2$, present in the unit cell. Ellipsoids show 30% probability levels. (B, bottom) Molecular structure of the second species of **2**, Nd[2,6-$(CH_2C_5H_4)_2$-C_5H_3N][μ-OS(O)O]$_2$, present in the unit cell. Ellipsoids show 30% probability levels.

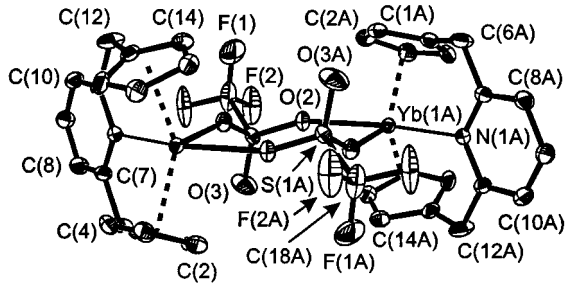

Figure 3. Molecular structure of **5**, Yb[2,6-$(CH_2C_5H_4)_2$-C_5H_3N][μ-OS(O)O]l_2. Ellipsoids show 30% probability levels.

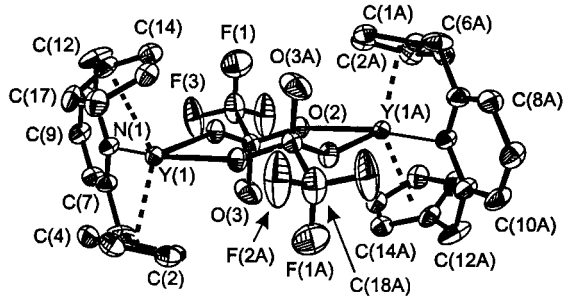

Figure 4. Molecular structure of **4**, Y[2,6-$(CH_2C_5H_4)_2$-C_5H_3N][μ-OS(O)O]$_2$.

pattern as expected for the two diastereotopic methylene protons, only one broad singlet occurs (δ 4.17). According to a VT ^{1}H NMR study between 296 and 193 K (see the following section), two different isomers of **4** seem to interconvert at room temperature rapidly on the NMR time scale. Thus, at 193 K (Figure 5a) the spectral patterns of two similar, but not equal, species are more clearly apparent.

In fact, at lower temperature, the protons of the pyridyl units of **4** give rise to two triplets (4-position) and two doublets (3- and 5-positions), suggesting that below room temperature two isomers (with two virtually equal C_5H_3N fragments each) coexist. The changes occurring in the spectral ranges of the Cp protons and methylene protons, respectively, are less clear-cut. Thus, at 193 K (Figure 5b) six (instead of eight) signals of different intensities and line widths appear in the Cp range, while in the CH_2 range one intense singlet seems to partially overlap with at least one multiplet.

The paramagnetic complexes **1**−**3** and **5** likewise give rise to ^{1}H NMR spectra consistent with the assumption of fluxional systems (see the Experimental Section). Thus, the number of observable signals is approximately doubled when the temperature is lowered. However, owing to the usual impact of paramagnetic central metal ions (as reflected by notable line broadening and significant signal displacement, collapse of multiplet splitting, etc.), reliable assignments have so far not always been possible.

Because of the more pronounced chemical shift differences owing to the presence of paramagnetic metal ions, the coalescence temperature of the dynamic systems are raised above the coalescence temperature of a diamagnetic system.[14] One striking example is provided by the VT ^{1}H NMR spectra of the ytterbium(III) complex **5** (see the Experimental Section). Here already the room-temperature spectrum displays two groups of signals of different intensity that might tentatively be ascribed to the two isomeric species of **4**, the individual sets of signals of which emerge only at a notably lower temperature.

5. Extended Variable-Temperature ^{1}H and ^{19}F NMR Study of 4

The VT ^{1}H spectra of **4** have been examined critically with regard to the static X-ray structure (Figure 4) and to the scheme depicted in Figure 6. The O−Y−O units in the eight-membered $Y_2S_2O_4$ ring define two planes which are almost parallel. The S atoms are below and above these planes, i.e., with reciprocal trans orientation. The more bulky CF_3 substituents at sulfur are along the less hindered equatorial orientations, while the oxygen atoms occupy the axial orientations. The two L ligands bound to the Y atoms by N→Y bonds are coplanar with the adjacent O−Y−O plane and reciprocally trans oriented. We can tentatively assign the two sets of signals detected at low temperature to the above-described isomer (**4A**) and to its isomer (**4B**) having the two L ligands cis oriented. We can likewise assume that the most stable isomer present in solution is the crystallographically verified isomer (**4A**).

However, the ^{1}H spectrum at 193 K (Figure 5a) does not exactly conform to this view. In particular, the meta and para pyridine protons of each isomer are represented by 2:1 doublet:triplet systems, while in **4A** and **4B** the two protons in meta positions are nonequivalent. We can think of the (unlikely) possibility of casual isochronicity for the meta protons in *both* isomers or of the (more probable) possibility of a dynamic process which is not yet completely "frozen", with regard to signals characterized by small chemical shift differences.

(14) Steudel, A.; Siebel, E.; Fischer, R. D.; Paolucci, G.; Lucchini, V. *J. Organomet. Chem.* **1998**, *556*, 229.

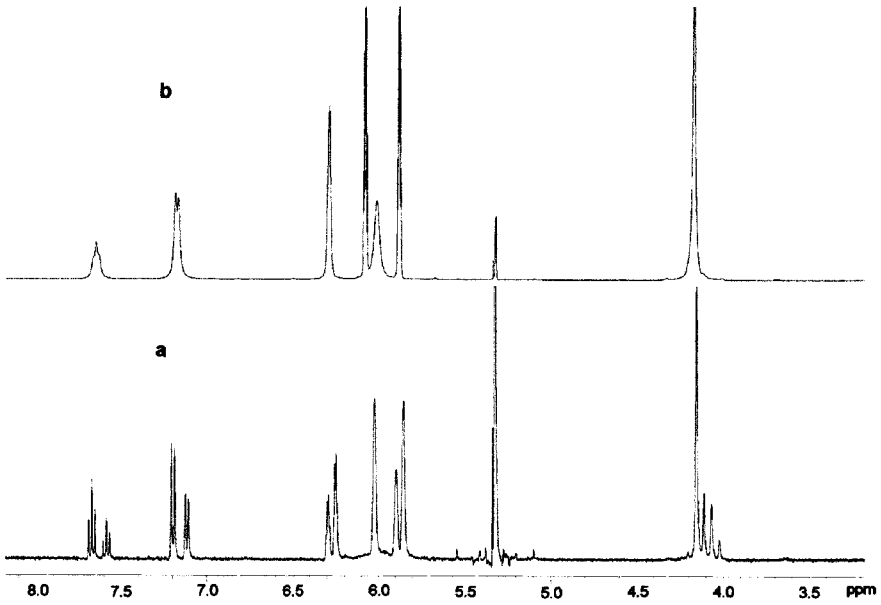

Figure 5. Variable-temperature ^{1}H NMR (400 MHz, CD_2Cl_2) spectra of Y[2,6-$(CH_2C_5H_4)_2$-C_5H_3N][μ-OS(O)O]$_2$: (a) at 193 K; (b) at 296 K.

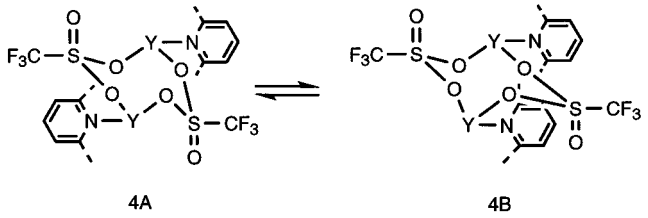

Figure 6. Schematic drawing of the equilibrium between the two isomeric forms of **4**. The two cyclopentadienyl rings are omitted for clarity.

In view of the difficulties in adopting the VT ^{1}H NMR results for a more detailed assessment, a solution of **4** in toluene-d_8 was also subjected to a VT ^{19}F NMR study, relying on the wider chemical shift range of this spectroscopy. As a matter of fact, in the temperature range between 305.3 and 267.9 K two sets of signals appear (Figure 7). One set consists of one comparatively intense singlet, which can only be attributed to a molecule with two transoid oriented pyridyl units. The two CF_3 groups could in principle be trans or cis positioned; in view of their trans orientation in crystalline **4** (vide supra) the singular ^{19}F resonance belongs most probably to the same molecular configuration as found in the solid state (**4A**). The second set of ^{19}F signals consists of a *pair* of equally intense singlets. Two ^{19}F resonances should appear only if the two pyridyl units would adopt a cisoid orientation, since then the two triflato bridges will become nonequivalent (**4B**). At this stage it remains unclear whether in the latter isomer the two CF_3 groups would be trans or cis oriented.

Looking at the assignments made in Table 4, the crystallographically proved structure (**4A**) is also the most stable one in solution. As the signals broaden continuously with increasing temperature, coalescence is finally expected, according to rapid interconversion of **4A** and **4B** on the NMR scale.

Although the collapse of the signals occurs at a temperature higher than that monitored, we could carry out a satisfactory line-shape analysis of the VT ^{19}F NMR spectra based on the DNMR5 program[15] for 11 different temperatures. Figure 7 shows the strong resemblance of the experimental and simulated spectra for the highest temperatures. An Eyring analysis of the resulting k values (Figure 8A) leads to the activation parameters $\Delta H^{\ddagger} = 12.9$ kcal mol^{-1} and $\Delta S^{\ddagger} = -4.2$ cal deg^{-1} mol^{-1}, while according to the van't Hoff equation (Figure 8B) the thermodynamic parameters of the two interconverting species differ as follows: $\Delta H° = 0.12$ kcal mol^{-1} and $\Delta S° = -0.3$ cal deg^{-1} mol^{-1}.

The most interesting feature arising from this analysis is the small absolute value of the activation entropy $\Delta S^{\ddagger}$. Because of the large intrinsic errors in the evaluation of entropy parameters from the intercept found for Eyring or van't Hoff plots, which involves an extrapolation to temperatures far away from the experimental ones, $\Delta S^{\ddagger}$ and $\Delta S°$ only become significant if their absolute values notably differ from zero.

In the present case, however, the experimental $\Delta S^{\ddagger}$ value must be considered to lie close to zero, and therefore neither features to be associated with high positive values (the cleavage or weakening of a bond in the transition state) nor features related to negative values (a more polarized transition state, with increased solvent ordering) seem to accompany the interconversion between the two isomeric forms **4A** and **4B**. Undoubtedly suitable ligand rearrangements around each yttrium atom devoid of a cleavage of the Y−N(pyridine) bond should then be postulated. In Figure 9 the orientation of the ligands both in the ground state (from the X-ray structure) and in the required transition state is shown. To a reasonable approximation, the ground-state arrangement is trigonal-bipyramidal, with the Cp units and one oxygen atom in an equatorial orientation and the pyridine nitrogen and a second oxygen atom in axial positions (Figure 9A). A Berry type turnstile twist could

(15) Stephenson, D. S.; Binsch, G. DNMR5, Quantum Chemistry Program Exchange; QCPE 365. Modified by: LeMaster, C, B,; LeMaster, C. L.; True, N. S. Quantum Chemistry Program Exchange; QCMP 059.

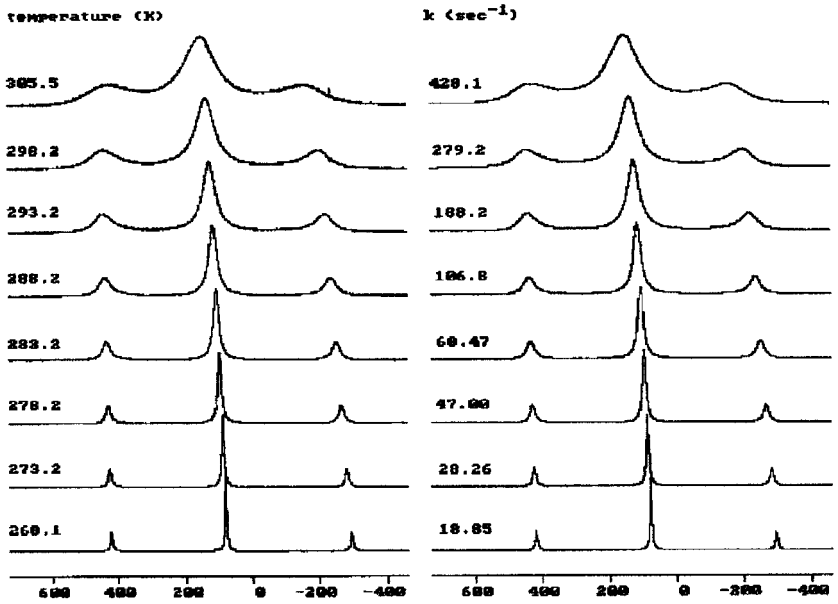

Figure 7. Experimental (left) and computer-simulated (right) ^{19}F NMR spectra of **4**. The scale (Hz) is referred to the resonance of the central singlet as measured at 193 K.

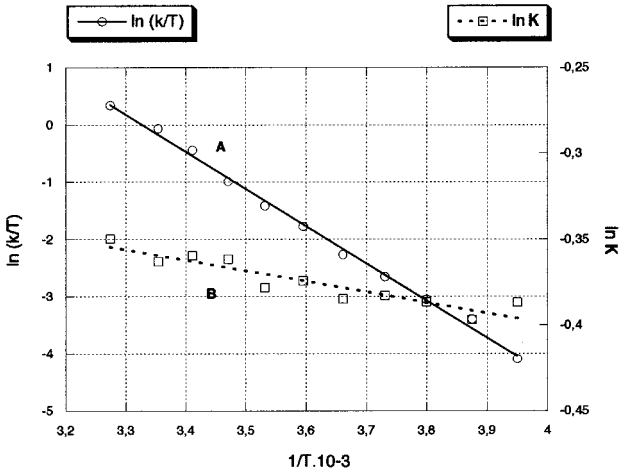

Figure 8. Eyring (A) and van't Hoff (B) plots for the equilibrium of the two interconverting species of **4** as obtained from the VT ^{19}F NMR data.

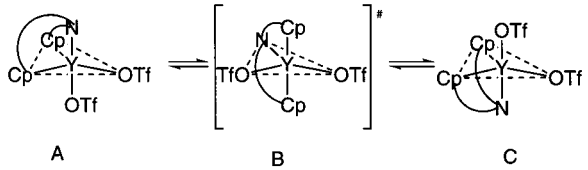

Figure 9. Schematic drawing of the possible mechanism involved in the interconversion of the two species of **4**.

Table 4. Mutual Orientations of the *ansa*-Dicyclopentadienyl and CF_3 Groups and the Corresponding ^{19}F NMR Signals

2,6-$(CH_2)_2C_5H_3N$	CF_3	^{19}F signals
transoid	trans	1
transoid	cis	1
cisoid	cis	2
cisoid	trans	2

lead to the postulated transition state, which is also trigonal bipyramidal, with the two Cp units in axial positions (Figure 9B). A subsequent Berry type rearrangement could then convert the molecule into another observable isomer with inverted (i.e. cisoid oriented) pyridine (Figure 9C).

6. Experimental Section

All operations were carried out in an atmosphere-controlled (N_2: 1 ppm of O_2 and <1 ppm of H_2O) automatic glovebox (M-BRAUN 200 GI) equipped with an internal refrigerator and facilities to carry out reactions at low and high temperatures. All chemicals were reagent grade and purified as required. THF and aromatic and aliphatic hydrocarbons were first dried by distillation from $LiAlH_4$ and then from potassium−benzophenone ketyl before use. CH_2Cl_2 was dried by distillation from CaH_2. Deuterated solvents were obtained from Cambridge Isotope Laboratories (all ≥99 atom % D) and were degassed (by freeze−thaw cycles) and dried over Na/K alloy (benzene-d_6, toluene-d_8, tetrahydrofuran-d_8) or P_2O_5 (CD_2Cl_2) before use. Anhydrous $[Ln(OTf)_3]$ (Ln = Pr, Nd, Sm, Y, Yb) were prepared from the corresponding metal oxides (Alfa Inorganics) and CF_3SO_3H (Aldrich).[16] Na_2L was prepared as previously described.[2]

^{1}H NMR spectra were recorded on either a Bruker A200 or a Varian Unity 400 spectrometer. VT ^{19}F NMR spectra were recorded on a Varian Unity 400 spectrometer. Chemical shifts were referenced to the proton resonances of the residual undeuterated solvent molecules.

Elemental analyses (C, H, N, S) were performed by the microanalytical laboratory of the Department of Chemistry (Perkin-Elmer 240B microanalyzer).

$[LPr(\mu\text{-}OTf)]_2$ (1). A solution of Na_2L (2.01 mmol) in tetrahydrofuran (20 mL) was added dropwise with magnetic stirring at room temperature to a solution of $Pr(OTf)_3$ (2.00 mmol) in anhydrous tetrahydrofuran (30 mL). The reaction mixture was stirred at room temperature for 12 h, whereafter the solvent was removed under vacuum and replaced by CH_2Cl_2 (20 mL). After filtration and addition of *n*-hexane to the green filtrate, green microcrystals of **1** precipitated (93% yield).

Anal. Calcd for $C_{18}H_{15}F_3NO_3PrS$: C, 41.32; H, 2.89; N, 2.68; S, 6.13. Found: C, 40.80; H, 3.00; N, 2.75; S, 6.35. ^{1}H NMR ($CDCl_3$, 200 MHz, δ (ppm)) at 296 K: 102.81 (bs, 2H, Cp), 35.25

(16) Steudel, A.; Fischer, R. D. In *Synthetic Methods of Organometallic and Inorganic Chemistry (Herrmann/Brauer;* Edelmann, F. T., Ed.; G. Thieme: Stuttgart, Germany, 1997; p 89.

(bs, 2H, Cp), 18.69 (bs, 4H, $-CH_2-$), 0.81 (bs, 2H, Py-3,5), −0.03 (bs, 1H, Py-4), −23.84 (bs, 2H, Cp), −49.50 (bs, 2H, Cp). ^{1}H NMR ($CDCl_3$, 200 MHz, δ (ppm)) at 193 K: 204.67, 79.21, 46.81, 40.57, −1.81, −3.70, −5.20, −53.38, −86.40.

[LNd(μ-OTf)]$_2$ (2). The light blue complex **2** was prepared by following the same synthetic procedure as previously reported for the Pr complex **1** (90% yield).

Anal. Calcd for $C_{18}H_{15}F_3NNdO_3S$: C, 41.05; H, 2.87; N, 2.66; S, 6.09. Found: C, 40.5; H, 3.05; N, 2.65; S, 6.45. ^{1}H NMR ($CDCl_3$, 200 MHz, δ (ppm)) at 296 K: 46.06 (bs, 2H, Cp), 15.41, 13.26 (bs, 4H, Cp), 5.78 (bd, 2H, Py-3,5), 5.09 (bt, 1H, Py-4), 3.25 (bs, 4H, $-CH_2-$), −24.24 (bs, 2H, Cp), −39.43 (bs, 2H, Cp). ^{1}H NMR ($CDCl_3$, 200 MHz, δ (ppm)) at 193 K: 96.72, 80.22, 31.34, 27.96, 23.89, 20.28, 4.25, 3.14, 2.24, −0.02, −8.82, −41.08, −50.33, −60.94, −79.66.

[LSm(μ-OTf)]$_2$ (3). The yellow complex was prepared by following the same synthetic procedure as previously reported for the Pr complex **1** (92% yield).

Anal. Calcd for $C_{18}H_{15}F_3NO_3SSm$: C, 40.58; H, 2.84; N, 2.63; S, 6.02. Found: C, 39.50; H, 3.00; N, 2.80; S, 6.30. ^{1}H NMR ($CDCl_3$, 200 MHz, δ (ppm)) at 296 K: 14.03 (bs), 10.60 (bs), 8.49(bs), 7.48 (bs), 7.19 (bs), 5.76 (bs), 5.67 (bs), 5.38 (bs), 2.04 (bs). ^{1}H NMR ($CDCl_3$, 200 MHz, δ (ppm)) at 193 K: 12.57, 12.30, 9.64, 8.60, 7.94, 7.73, 7.19, 7.07, 6.61, 6.52, 6.18, 6.08, 5.65, 5.56, 4.61, 4.52, −0.46, −0.75.

[LY(μ-OTf)]$_2$ (4). The white-yellow complex was prepared by following the same synthetic procedure as previously reported for the Pr complex **1** (95% yield).

Anal. Calcd for $C_{18}H_{15}F_3NO_3SY$: C, 45.87; H, 3.21; N, 2.97; S, 6.80. Found: C, 45.35; H, 3.40; N, 3.05; S, 7.15. ^{1}H NMR (CD_2Cl_2, 400 MHz, δ (ppm), J (Hz)) at 296 K: 7.65 (t, 1H, J = 7.11, Py-4), 7.18 (d, 2H, J = 7.10, Py-3,5), 6.29 (bq, 2H, J = 2.6, Cp), 6.08 (q, 2H, J = 2.6, Cp), 6.01 (bs, 2H, Cp), 5.88 (q, 2H, J = 2.6, Cp), 4.17 (bs, 4H, $-CH_2-$). ^{1}H NMR (CD_2Cl_2, 400 MHz, δ (ppm), J(Hz)) at 193 K: more abundant isomer, 7.67 (t, J = 7.7, Py-4), 7.20 (d, J = 7.7, Py-3,5), 6.25 (bq, J = 2.6, Cp), 6.03 (bs, Cp), 5.91 (bq, J = 3.3, Cp), 5.86 (bs, Cp), 4.15 (bs, CH_2); less abundant isomer, 7.59 (t, J = 7.7, Py-4), 7.12 (d, J = 7.7, Py-3,5), 6.30 (bq, J = 2.6, Cp), 5.96 (bs, Cp), 5.86 (bs, Cp) 4.13 (d, J = 18, CH_2), 4.04 (d, J = 18, CH_2).

[LYb(μ-OTf)]$_2$ (5). The orange complex was prepared by following the same synthetic procedure as previously reported for the Pr complex **1** (90% yield).

Anal. Calcd for $C_{18}H_{15}F_3NO_3SYb$: C, 38.93; H, 2.72; N, 2.52; S, 5.77. Found: C, 38.60; H, 2.90; N, 2.70; S, 6.15. ^{1}H NMR ($CDCl_3$, 200 MHz, δ (ppm)) at 296 K: 135.54 (bs), 19.07(bs), 12.02 (bs), 8.03 (bs), 1.32(bs), −14.56(bs),-26.68 (bs), −30.72 (bs), −31.2 (bs,), −45.39 (bs), −61.76 (bs), −139.72 (bs). ^{1}H NMR ($CDCl_3$, 200 MHz, δ (ppm)) at 193 K: 286.12 (bs), 32.33 (bs), 19.77 (bs), 11.92 (bs), 10.80 (bs), 6.58 (bs), 4.08 (bs), 3.04 (bs), −5.82 (bs), −23.95 (bs), −28.87 (bs), −57.10 (bs), −62.88 (bs), −65.58 (bs), −75.0 (bs), −96.68 (bs), −129.51 (bs), −137.35 (bs), −244.81 (bs).

X-ray Crystal Structures. Single crystals of **2** were grown within 5 days from a concentrated solution in toluene/methylene chloride (4:1) at a temperature of ca. 5 °C. Crystals of **4** and **5** deposited when concentrated (at ca. 100 °C!) toluene solutions were cooled slowly to room temperature. The determination of the lattice parameters and the subsequent measurements of intensity data were carried out at low temperature. Data were collected for **2** and **5** at 153 K on a Hilger & Watts Y 290 diffractometer (Mo Kα radiation and graphite monochromator), and for **4** at 173 K on an Enraf-Nonius CAD 4 diffractometer (Cu Kα radiation). Heavy atoms were located by three-dimensional Patterson synthesis, and subsequent difference Fourier and least-squares calculations led to the positions of the C and O atoms.[17] Cyclopentadienyl rings were refined anisotropically. For all structures an empirical absorption correction was conducted, using the DIFABS strategy,[18] as implemented in the PLATON software package.[19]

Acknowledgment. G.P, J.Z., and V.L. are indebted to Dr. S. Formenti for help in the synthesis of the complexes and to the Italian Ministry of the University and of the Scientific and Technological Reasearch (MURST) for the financial support of PRIN-98 (Research Program of National Interest) "Stereoselective Polymerizations: New Catalysts and New polymeric materials".

Supporting Information Available: Tables giving crystallographic data for compounds **2**, **4**, and **5**; data are also available in CIF format. This material is available free of charge via the Internet at http://pubs.acs.org. Full details of the crystal structure determinations of **2** and **4** have been deposited at the Cambridge Crystallographic Data Centre, 12 Union Road, Cambridge CB2 1EZ, U.K. (http://www.ccdc.cam.ac.uk) and can be obtained on quoting the depository numbers CCDC 132897 and CCDC 118681, respectively. The details of the crystal structure of **5** have been deposited at the Fachinformationzentrum Karlsruhe, GmbH, D76344 Eggenstein-Leopoldshafen, Germany, and can be obtained on quoting the depository number CSD 408874.

OM0104868

(17) Sheldrick, G. M. SHELXL93: Program for the Refinement of Crystal Structures; University of Göttingen, Göttingen, Germany, 1993. Sheldrick, G. M. SHELXTL-PLUS, Release 4.21/V; Siemens Analytical X-ray Instruments Inc., Madison, WI, 1993.

(18) Walker, N.; Stuart, D. *Acta Crystallogr.* **1983**, *A39*, 158.

(19) Spek, A. L. *Acta Crystallogr.* **1990**, *A46*, C34 (Version 12.05.99, 32 bit Windows Implementation by Louis J. Farrugia).